This document is confidential and is proprietary to the American Chemical Society and its authors. Do not copy or disclose without written permission. If you have received this item in error, notify the sender and delete all copies.

Investigation of the unusual ability of the [FeFe] Hydrogenase from *Clostridium beijerinkii* to access an O₂protected state.

Journal:	Journal of the American Chemical Society
Manuscript ID	ja-2020-04964n.R1
Manuscript Type:	Article
Date Submitted by the Author:	18-Jun-2020
Complete List of Authors:	Corrigan, Patrick; Pennsylvania State University, Chemistry Tirsch, Jonathan; Pennsylvania State University, Chemistry Silakov, Alexey; Pennsylvania State University, Chemistry



Investigation of the unusual ability of the [FeFe] Hydrogenase from *Clostridium beijerinkii* to access an O₂-protected state.

Patrick S. Corrigan¹, Jonathan L. Tirsch¹, and Alexey Silakov^{1,*}

¹ Pennsylvania State University, 104 Chemistry Building, University Park, PA, 16802, USA

ABSTRACT

[FeFe] hydrogenases are enzymes capable of producing and oxidizing H₂ at staggering submillisecond time scales. A major limitation in applying these enzymes for industrial hydrogen production is their irreversible inactivation by oxygen. Recently, an [FeFe] hydrogenase from Clostridium beijerinckii (CbHydA1) was reported to regain its catalytic activity after exposure to oxygen. In this report, we have determined that artificially matured CbHydA1 is indeed oxygen tolerant in the absence of reducing agents and sulfides by means of reaching an O₂-protected state (H_{inact}). We were also able to generate the H_{inact} state anaerobically via both chemical and electrochemical oxidation. We use a combination of spectroscopy, electrochemistry, and density functional theory (DFT) to uncover intrinsic properties of the active center of CbHydA1, leading to its unprecedented oxygen tolerance. We have observed that reversible, low-potential oxidation of the active center leads to the protection against O₂-induced degradation. The transition between the active oxidized state (H_{ox}) and the H_{inact} state appears to proceed without any detectable intermediates. We found that the H_{inact} state is stable for more than 40 hours in air, highlighting the remarkable resilience of CbHydA1 to oxygen. Using a combination of DFT and FTIR, we also provide a hypothesis for the chemical identity of the H_{inact} state. These results demonstrate that CbHydA1 has remarkable stability in the presence of oxygen, which will drive future efforts to engineer more robust catalysts for biofuel production.

KEYWORDS: [FeFe] hydrogenase, Oxygen tolerance, Fourier Transform Infrared spectroscopy, Electrochemistry, Density Functional Theory

INTRODUCTION

The search for renewable energy carriers that do not lead to further anthropogenic climate change is a major modern technological challenge. Steam reforming is a common method to produce hydrogen, but it utilizes fossil fuels such as methane and produces carbon dioxide. Therefore, it is of vital importance not only to find a way to produce hydrogen from renewable, carbon-free sources, but also to find an efficient catalyst that reduces the intake of energy required to make hydrogen. Hydrogenases are highly active enzymes capable of producing and oxidizing hydrogen. The two main classes of hydrogenases are the [FeFe] and [NiFe], named after the metal content of their active site. The work presented here focusses on the former. [FeFe] hydrogenases (HydA) are capable of producing up to 7,500 H₂ molecules per second at ambient temperature and neutral pH in aqueous media.^{2–5} These properties make them promising catalysts to target for carbonneutral hydrogen production.

Figure 1 shows a schematic representation of the active center of the [FeFe] hydrogenase (H-cluster) and a simplified catalytic cycle. The H-cluster consists of two subclusters known as the [4Fe-4S]_H "cubane" and the di-nuclear [2Fe]_H. The mixed ligation of carbon monoxides and cyanides of the [2Fe]_H keeps the di-iron core in a low-valent, low-spin state. The amine in the bridging azadithiolate moiety (ADT) has been proposed to serve as a kinetically fast base. Ref. Ref. The distal iron (Fe_d) in the [2Fe]_H cluster is the hydrogen-binding site. In vivo, three maturation factors (HydE, HydF, and HydG) activate HydA. Ref. However, it is possible to incorporate the H-cluster in the apo-HydA (containing only the [4Fe-4S] clusters) in vitro using a synthetic di-iron compound [Fe₂(μ -adt)(CO)₄(CN)₂]²⁻ (adt = [S₂C₂H₄NH]²⁻). The resulting holo-HydA is phenotypically indistinguishable from natively-matured enzymes. Ref. In addition to the H-cluster, many [FeFe] hydrogenases contain additional auxiliary [4Fe-4S] and [2Fe-2S] iron-sulfur clusters called F-clusters.

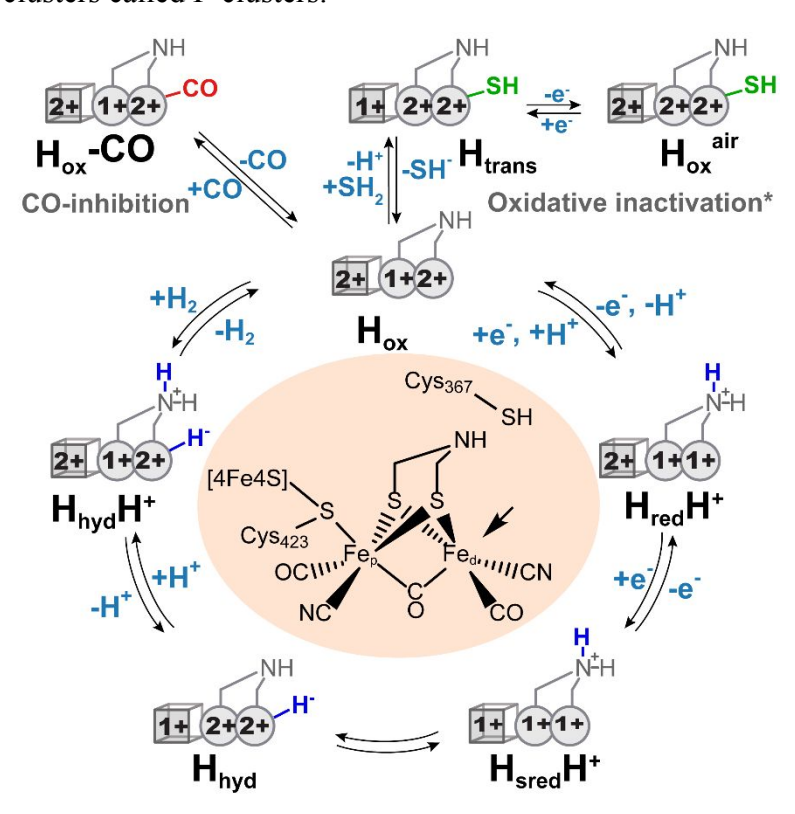


Figure 1. Simplified representation of the proposed catalytic and inhibitory pathways in [FeFe] hydrogenases. The [4Fe-4S]_H is represented as a cube, and the two iron atoms of the [2Fe]_H are represented as spheres. The formal oxidation state of any metal center is written directly over the metal center in question. The chemical structure of the H-cluster is shown in the center of the cycle. Arrow points at the open coordination site. *Oxidative inactivation is depicted as proposed for DdHydAB^{6,10}.

In the presence of O₂, the majority of [FeFe] hydrogenases irreversibly inactivate. It is generally accepted that the reaction proceeds via the reduction of O₂ to form reactive oxygen species (ROS) through oxidation of the H-cluster. Consequently, the ROS generated attack components of the H-cluster leading to an irreversible degradation of the active metallocofactor.^{23,25–28} A low level of degradation results in the appearance of the CO-inhibited form of the H-cluster (H_{ox}-CO) in EPR and FTIR spectroscopic techniques.^{12,29} Prolonged exposure to oxygen results in the complete

degradation of the H-cluster, and causes the disappearance of any spectroscopic signatures associated with the [2Fe]_H subcluster. ^{12,26,27} Using algal [FeFe] hydrogenase from *Chlamydomonas reinhardii* (*Cr*HydA1), Swanson et al. ²⁶ observed that exposure to oxygen *in crystallo* results in the oxidation of the non-coordinating cysteine residue that is neighboring the open coordination site of the H-cluster to sulfinic acid. O₂-exposure *in crystallo* of the [FeFe] hydrogenase I from *Clostridium pasteureanum* (*CpI*) by Esselborn et al. ²⁵ resulted in the depletion of electron density primarily within the [2Fe]_H subcluster. The authors also noted that in the absence of the [2Fe]_H subcluster, degradation of the metalloclusters is minimal, indicating that the presence of the complete H-cluster is instrumental to the generation of the ROS species. Systems containing multiple F-clusters, i.e. *CpI* or *C. acetobutylicum* (*Ca*) HydA, appear to be more oxygen tolerant than those lacking F-clusters, i.e. *Cr*HydA1. ^{27,30} The difference is especially noticeable in protein film voltammetry experiments (PFV). However, this paradigm has been challenged recently when it was observed that deletion of F-clusters did not lead to noticeable differences in the unusually slow O₂-dependent inactivation rate of *Megasphera elsdenii* (*Me*) HydA. ³¹

Until recently, oxygen-stable forms were only observed in [FeFe] hydrogenases from the sulfate-reducing bacteria *Desulfovibrio desulfuricans* (DdHydAB) and *Desulfovibrio vulgaris* Hildenborough (DvHydAB). Aerobically purified DdHydAB and DvHydAB exhibit an inactive, oxygen-stable form called H_{inact} . ^{12,29} Once activated under a hydrogen-rich atmosphere or with chemical reductants, these enzymes lose the ability to access the H_{inact} form and become susceptible to oxidative degradation similar to other HydA enzymes. One-electron reduction of the H_{inact} state of DdHydAB generates an intermediate state termed H_{trans} . The H_{trans} state exhibits an EPR spectrum characteristic of a [4Fe-4S]¹⁺, indicating the reduction of the [4Fe-4S]_H subcluster rather than the [2Fe]_H (see Figure 1). ^{6,12,29}

Rodríguez-Maciá et al. 6 were able to regenerate the inactive state (designated as H_{ox}^{air} in this work) in DdHydAB by adding sodium sulfide to the active enzyme and reacting it with a mild oxidant (hexamine ruthenium (III) chloride, HAR). The IR spectra obtained for the resulting state was identical to the one captured natively. Recent structural characterization of the H_{ox} air state of DdHydAB unequivocally showed the presence of a sulfur ligand bound to the open coordination site. 10 When in this state, the protein was able to withstand exposure to air for approximately 50 hours, with about 50% loss of the H-cluster-specific IR signal. ⁶ Rodríguez-Maciá et al. were also able to access a similar sulfide-generated, O₂-tolerant state in the algal hydrogenase CrHydA. However, sulfide-aided oxidative treatment of clostridial hydrogenase CpI did not result in the H_{ox} air state. The authors proposed that H₂S originating from Na₂S is deprotonated to HS⁻ upon binding to the H-cluster. This binding results in a charge rearrangement within the H-cluster, resulting in the H_{trans} state. Oxidation of the H_{trans} state by one electron leads to the H_{ox} air state. Conversion of the H_{trans} state to the H_{ox} state requires a one-electron reduction of the enzyme and does not appear to be associated with the H-cluster. Instead, one of the F-clusters is likely reduced, which causes a transition of the H-cluster from H_{trans} to H_{ox} due to redox anti-cooperativity.^{6,7} This important finding illustrated that the H-cluster could be protected from oxygen by anaerobic oxidation in the presence of a small, non-inhibiting molecule such as H₂S.

In 2016, Morra et al. ³² provided evidence that an [FeFe] hydrogenase from *Clostridium beijerinckii* (termed CbA5H) can fully recover its activity after a prolonged (10 min) exposure to air. Here we will refer to this enzyme as CbHydA1, following the commonly used notation for this class of hydrogenases and accounting for the presence of multiple [FeFe] hydrogenases in C.beijerinckii strains. The authors obtained similar rates of catalysis pre- and post-exposure to air in both H₂ evolution and H₂ oxidation in vitro assays. FTIR spectroscopic experiments demonstrated that the CbHydA1 enters an inactive state when exposed to air. The obtained spectrum was similar to the H_{ox} air spectrum observed in *Dd*HydAB and *Cr*HydA1, albeit with noticeable shifts in the vibrational modes for the CO-ligands. To differentiate the inactive states, we will designate "H_{ox} air" for the inactive state obtained in the presence of sulfides per Rodríguez-Maciá et al.⁶ and "H_{inact}" as the inactive state obtained in CbHydA1 per Morra et al. 32 Under reducing conditions, the H_{inact} state converts to either the H_{ox} or $H_{red}H^+$ states. Morra et al.³² were able to generate a pure H_{ox} -CO state by exposing the active enzyme to CO gas. However, the H_{ox}-CO state does not accumulate under oxidative treatment. Unfortunately, as the authors performed O₂ exposure in the presence of sodium dithionite, it is unclear whether this strong reductant facilitates the reported O₂-tolerance of *Cb*HydA1.

In light of the work of Rodríguez-Maciá et al.^{6,10}we sought to investigate further this intriguing case of what could potentially be the first example of an oxygen-tolerant [FeFe] hydrogenase. In this work, we present a spectroscopic and electrochemical investigation of *Cb*HydA1. Our investigation shows that *Cb*HydA1 can indeed safely and reversibly react with oxygen leading to an inactive, O₂-protected H_{inact} state. The process does not depend on sodium dithionite or Na₂S. In our experiments, the conversion to the H_{inact} state is favorable at surprisingly low redox potentials. Aerobic or anaerobic oxidative treatment results in the same H_{inact} state in *Cb*HydA1. In the active state, the H-cluster of *Cb*HydA1 has nearly identical spectroscopic signatures to other well-studied enzymes of this family. However, the IR signatures of the H_{inact} state and the electrochemical properties of the H-cluster reveal differences that suggest a novel mechanism of oxygen tolerance.

RESULTS

Effect of air exposure on the activity of CbHydA. To conclusively verify the ability of CbHydA1 to restore activity after O_2 exposure, we performed rigorous testing in which multiple aliquots of the enzyme were repeatedly exposed to air and reactivated back by exposure to 100% hydrogen. We tested CbHydA1 for hydrogen oxidation using the standard methyl viologen reduction assay. To ensure the complete absence of any oxygen-scavenging reagents in our experiments, we removed the reducing agents as well as any sources of sulfides by desalting columns after Fe/S reconstitution and after activation with the CbHydA1 with the synthetic complex (see materials and methods). Some degradation is expected in prolonged experiments even in strictly anaerobic conditions and at 4 °C. To avoid any skew of the results due to the long-term gradual deterioration of the samples, we ensured that each aliquot experiences the same bench-time from start to finish. Aliquots of CbHydA1 to remain anaerobic were treated identically to air-treated aliquots except for incubating with 95% N_2 :5% H_2 gas instead of air for the same amount of time. In a given experiment, one aliquot was kept anaerobic, another aliquot was exposed once to air for 15

minutes, and the third aliquot was exposed twice to air (for 15 minutes each time). After each 15 min cycle, samples were exposed to pump-purge cycles with 100% H₂ for 15 min and then incubated under 1 atm H₂ for another 45 min, which results in complete activation of *Cb*HydA1 (see below). We applied the same H₂ treatment to all samples regardless of whether treated with air or with 95% N₂:5% H₂ gas. Air exposure was achieved by taking the *Cb*HydA1sample outside of the glovebox and incubated in open air at 4°C with continuous stirring.

The anaerobic control exhibited a specific activity of $218 \pm 50 \, \mu mol \, H_2 \cdot min^{-1} \cdot mg^{-1}$ for hydrogen oxidation. Samples incubated only once in air showed, on average, 40% reduction of activity (129 \pm 44 $\mu mol \, H_2 \cdot min^{-1} \cdot mg^{-1}$) and samples incubated twice with air were about four times less active than the anaerobic control (53 \pm 14 $\mu mol \, H_2 \cdot min^{-1} \cdot mg^{-1}$). Figure S5 shows typical time dependencies of methyl viologen reduction observed during these activity assays. This observation differs from the report by Morra et al.³², where the authors reported full recovery of enzymatic activity after exposure to oxygen and subsequent reactivation with hydrogen. We attribute this difference to the rigorous removal of oxygen-scavenging agents in our experiments.

Despite observing some decay, these results are unprecedented for [FeFe] hydrogenases. For instance, Baffert et al.³⁰ showed that exposure of CaHydA to short "bursts" of atmospheric concentrations of O_2 drastically and irreversibly degrades H_2 -oxidation catalytic current in PFV. CaHydA degrades completely after prolonged exposure to air.²⁷ Irreversible loss of catalytic current was observed in "burst" exposures to $\leq 25 \, \mu M$ of O_2 for $Megasphaera\ elsdenii\ HydA.³¹ Similar "burst" exposures of <math>Cr$ HydA to O_2 result in a complete loss of activity in a matter of minutes, as detected by PFV.^{23,27,31} To our knowledge, no reports exist on the recovery of enzymatic activity in any [FeFe] hydrogenase (other than CbHydA1) after exposure to O_2 in vitro, only in PFV experiments. In contrast, in our experiments, samples of CbHydA1 retain a substantial amount of activity *in vitro* after more than 15 min exposure to air, encouraging further investigation of this system.

Aerobic inactivation and stability. We proceeded with investigating the aerobic inactivation further. Fourier-transform IR spectra of [FeFe] hydrogenase in the 2120 - 1780 cm⁻¹ region consist of well-resolved CO/CN⁻ stretching bands with peak-positions sensitive to the electronic structure of the H-cluster. Therefore, we performed FTIR experiments to identify the steady-state species of *Cb*HydA1 upon various treatments. In our experiments, the as-prepared *Cb*HydA1 sample exhibits a definitive set of signals characteristic for the H_{ox} and H_{red}H⁺ states (see Figure 2A). The frequency of respective CO and CN⁻ IR bands are virtually identical to that of *Dd*HydAB (see Table S1).^{2,12} It is worth noting that we were not able to obtain a pure H_{red}H⁺ state by prolonged exposure to 100% H₂. Instead, some fraction of the enzyme remained in the H_{ox} state, which suggests the bidirectional nature of *Cb*HydA1.

In the presence of 1 atm of O_2 or air, the IR spectrum collapses into one well-defined set of peaks assigned to the inactive state, H_{inact} (see Figure 2D and Figure S6).³² Incubation with 1 atm of 100% H_2 for an hour fully reactivates the enzyme as indicated by the presence of the H_{ox} and $H_{red}H^+$ states (see Figure 2B). These results are consistent with the previously reported observations, i.e., CbHydA1 safely reacts with oxygen by transitioning into the H_{inact} state and can be reactivated with hydrogen. It is again worth stressing that we performed all experiments in the

absence of sodium dithionite and sodium sulfide, which were removed after enzyme isolation and activation by extensive desalting with PD-10 column (see Materials and methods section in the SI).

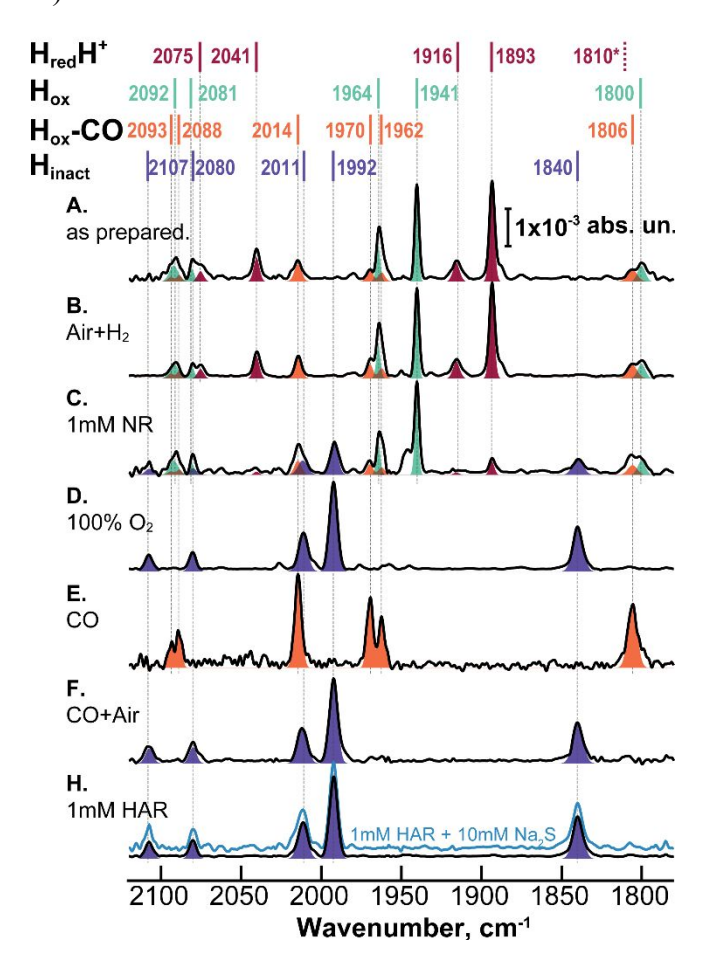


Figure 2. Transmission FTIR measurements of CbHydA1 at room temperature (black). **A.** As-prepared sample, **B.** Air-exposed (for 15 min) sample reactivated using incubation of H₂ gas for 1 hour. **C.** Sample A treated with 1 mM neutral red (NR), **D.** Sample A incubated under 100% O₂ atmosphere for 20 min. **E.** Sample A incubated under 100% CO atmosphere for 15 min, **F.** Sample E exposed to air for 15 min, **H.** Sample A treated with 1 mM HAR. Blue trace is a spectrum of CbHydA1 prepared in the same fashion but in the presence of 10 mM of Na₂S. Color bars and shaded areas depict the following states: $H_{red}H^+$ (maroon), H_{ox} (teal), H_{ox} -CO (orange), H_{inact} (purple). Corresponding band positions are indicated above the experimental traces. The asterisk indicates a possible location of the bridging CO band in the $H_{red}H^+$, per Birrel et al.³³

We were also able to generate a state spectroscopically-indistinguishable from H_{inact} using a mild oxidant, hexamine ruthenium (III) chloride (HAR) under strictly anaerobic environment (Figure 2H). To parallel the experiments by Rodríguez-Maciá et al.⁶ we oxidized the enzyme with 1mM HAR in the presence of 10mM Na₂S without any noticeable change to the resulting spectrum of the H_{inact} state (Figure 2H, red trace). In an attempt to generate pure H_{ox} state, we incubated CbHydA1 with 1 mM neutral red (NR, E_0 = -363 mV vs. NHE at pH 7.4). Surprisingly, this resulted in a mixture of the H_{ox} and the H_{inact} states, indicating an unexpectedly low redox potential of inactivation (Figure 2C). In these experiments, we have not observed any definitive signs of an H_{trans} -like state found in the process of oxidative inactivation and reactivation of the DdHydAB.

However, due to the complexity of the IR spectrum of the NR-treated CbHydA1, we cannot completely exclude the presence of small amounts of H_{trans} .

To verify the stability of CbHydA1 in the inactive state, we performed a stability test wherein 10 μ L of 100 μ M of CbHydA1 at pH 7.4 was exposed to air for a prolonged period in a home-made attenuated total reflectance (ATR) IR cell at room temperature (see Figure S2). After 42 hours at room temperature, we observed roughly a 22% decrease of the IR bands of the H_{inact} states without a noticeable appearance of any other signals (see Figure 3). Based on these observations, we suggest that the decrease in the activity of the enzyme observed in our experiments (see above) was due to processes preceding the formation of the inactive state. Once in the H_{inact} state, the system appears to be extremely stable.

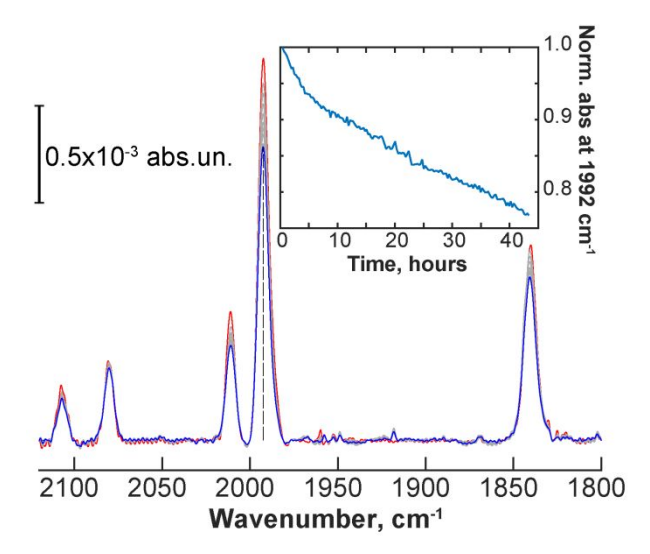


Figure 3. Long-term stability of *Cb*HydA1 exposed to air in ATR FTIR experiments. The red line is the first FTIR spectrum taken immediately after exposure, gray lines are intermediate spectra, and the blue line is the final spectrum taken after 42 hours. The inset shows changes in the absorbance at 1992 cm⁻¹ over time. Experimental conditions: 0.5 mM of *Cb*HydA1 in 50 mM HEPES, 300 mM KCl at pH7.4, 1 atm of air, room temperature, spectra recorded with 2 cm⁻¹ FTIR resolution with 1000 scans each.

To better understand the extent of degradation of CbHydA1, we compared IR spectra of two aliquots of the same sample in the inactive state prepared by exposure to O_2 and by anaerobic oxidation using HAR. The O_2 -treated sample appears to have roughly 20% less H_{inact} signal in IR than the anaerobic HAR-treated sample. This difference is noticeably smaller than the decay of the activity observed in methyl viologen reduction assays (see above). Furthermore, the overall decrease in the FTIR signal coincides with an appearance of an EPR signal at g = 4.29, which is a hallmark of adventitiously bound ferric iron originating from oxidative degradation of iron-sulfur clusters (see Figure S6).³⁴ There is also an apparent presence of a g = 2.01 signal characteristic of a [3Fe4S] cluster, corroborating the degradation of [4Fe-4S] clusters in CbHydA1 in the presence of O_2 . Together, these results suggest that the mild degradation of the accessory [4Fe-4S] clusters in the process of inactivation may contribute to the decrease in the enzymatic activity due to the disruption of the electron-transfer pathway. However, the outstanding long-term stability of the inactive CbHydA1 under aerobic conditions indicate that once oxidized, the accessory [4Fe-4S]

cofactors also become tolerant to O_2 . Future investigations into the structure and electronic properties of these [4Fe-4S] clusters will be required to fully explain this phenomenon.

Intriguingly, during these experiments, we did not observe an increase in the H_{ox} -CO state, which would be associated with the CO-inhibition of the still-intact molecules of the CbHydA1 by carbon monoxide released from the degraded H-cluster. Degradation of one H-cluster releases three CO molecules that can potentially inhibit up to three still-active hydrogenase enzymes. This effect was observed in the past for a variety of [FeFe] hydrogenases. 12,26 The presence of the H_{ox} -CO state is typically pronounced even with extremely mild oxidation. 12,26,35 Since it has been shown that the installation of the external CO ligand facilitates protection against O_2 attack on the H-cluster, 30,36 we expected that the CO-inhibited state would persist to some degree when the sample is exposed to O_2 . We can eliminate the possibility of exogenous CO not being able to interact with the H-cluster because exposure to 1 atm CO results in a pure H_{ox} -CO state (see Figure 2E). However, the reaction of the CbHydA1 in the pure H_{ox} -CO state with air resulted in a complete conversion of the enzyme into the H_{inact} state (see Figure 2F).

The results of our CO experiments are significant for two reasons. First, as the CO-treatment results in the pure H_{ox} -CO state, we have no reason to believe that such a diatomic molecule as O_2 cannot enter the active site. Second, these results indicate the ease with which the external CO ligand dissociated during the oxidation of the H-cluster. As the position of the CO bands in the IR spectra of the H_{ox} -CO state of CbHydA1 are practically identical to the ones observed earlier for DdHydAB or CrHydA1, we can rule out the possibility of any differences stemming from the strength of the coordination of the external CO to the H-cluster. Thus we expect that O_2 competition for binding at the active site will also be in favor of CO as it seems to be for other [FeFe] hydrogenases. 12,26 Consequently, it seems plausible that H_{ox} -CO conversion to H_{inact} is a result of facile oxidation of the H-cluster. Based on these considerations, we hypothesized that the transformation of the H-cluster to the H_{inact} state is a favorable outcome in a mildly electron-poor environment regardless of the state of the enzyme.

IR spectroelectrochemistry of *CbHydA*. The appearance of the H_{inact} state upon treatment of *CbHydA1* with NR (see above) indicate an unexpectedly low potential for inactivation. Therefore, we set to investigate the electrochemical properties of this H-cluster further by FTIR-spectroelectrochemistry. We constructed a purpose-built gas-tight FTIR cell that allows for electrochemical titrations simultaneously with IR detection under anaerobic conditions (see materials and methods). We identified IR spectra of four distinct states: H_{inact} , H_{ox} , $H_{red}H^+$, and a state very similar to H_{hyd} observed in *CpI*, *DdHydAB*, and *CrHydA1* (see Figure 4, Figure S7 and Table S1).^{37–39}. The observed H_{inact} state is spectroscopically identical to the H_{inact} state observed in the air-exposed *CbHydA*, confirming that this state can be accessed in the absence of oxygen (see Figure 4).

Rather intriguing is the process of electrochemical inactivation/reactivation. The transition of the H_{ox} state to the H_{inact} state and back appears to proceed directly. We have not observed any evidence for the inactive intermediate state (H_{trans}) found in DdHydAB (see Figure 4). We would like to note that even if the redox midpoint potentials for H_{trans}/H_{inact} and H_{ox}/H_{trans} were the same, H_{trans} must incubate to a detectable amount. This is because $E_0^{trans/inact} = E_0^{ox/trans}$ transpire

equivalent rates of the two redox transitions at any given potential (assuming no significant change in the electrode-protein electron transfer rates). 40 In the case of DdHydAB, both H_{ox}/H_{trans} and H_{trans}/H_{inact} redox transitions appear as one-electron transitions 6,12 , meaning two oxidizing equivalents are needed to achieve the transition from H_{ox} to H_{inact} (only one of these transitions is associated with the H-cluster). However, in the present case of CbHydA1, the H_{ox}/H_{inact} transition is well fitted to an n=1 Nernstian curves. Two sequential electron transfer processes would result in an n=2 electron process of H_{ox}/H_{inact} transition, which is not the case for CbHydA1. In line with our expectations from experiments with NR, the oxidative inactivation and reductive activation happen at an unusually low potential. A comparison between experiments performed at pH 7.4 and pH 8.4 showed that inactivation/reactivation mid-point potential has a mild pH dependence (-357 mV vs. NHE and -383 mV vs. NHE, respectively) (see Figure 4 and Figure S7). Therefore, it is likely that electrochemical inactivation of CbHydA1 proceeds directly from H_{ox} to H_{inact} states and only requires oxidation of the H-cluster by one electron.

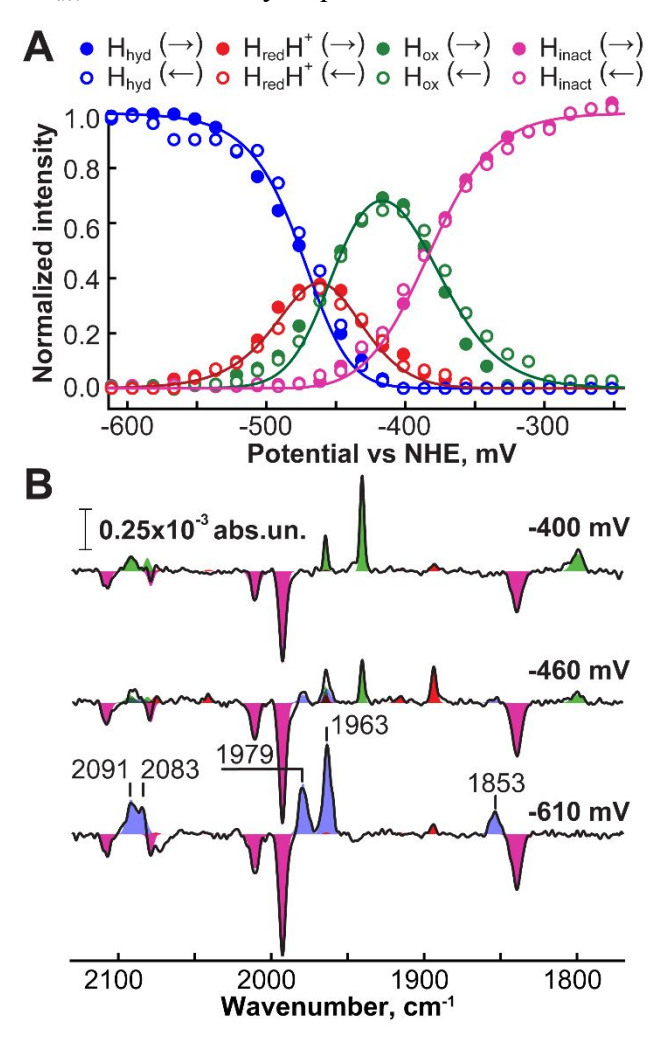


Figure 4: FTIR-spectroelectrochemical titration of *Cb*HydA1 at pH 8.4. A) Dependence of population of H_{inact} (magenta), H_{ox} (green), H_{red}H⁺ (red) and H_{hyd} (blue) states on the applied potential. Filled circles represent oxidative scans, and empty circles represent reductive scans. Solid lines are fits to Nernstian equations with n=1 and E₀hyd/red= -466 \pm 5mV vs NHE, E₀red/ox=-455 \pm 5mV vs NHE, E₀ox/inact=-383 \pm 5mV vs NHE. B)

Representative difference FTIR spectra obtained by subtracting -400 mV vs NHE, -460 mV vs NHE and -610 mV vs NHE spectra with the -200mV vs NHE spectrum. Both panels use the same color-coding. Numbers above the lower spectrum designate bands assigned to the H_{hyd} state. Positions of other bands highlighted are identical to those indicated in Figure 2.

Interestingly, at low potentials, we observed the conversion of the $H_{red}H^+$ state into what appears to be the hydride-bound state (H_{hyd}). This is surprising as the H_{hyd} state is not known to accumulate under conditions used in these experiments. Also, the conversion occurs, without any noticeable accumulation of the super-reduced state, previously reported to form in wild-type CrHydA and DdHydAB in similar experiments (no such state was reported for CpI or any other clostridial species). The IR bands observed for the low-potential state closely match bands associated with H_{hyd} in CrHydA and DdHydAB (see Figure 1 and Table S1). The conversion seems to follow a one-electron reduction/oxidation behavior with a pH dependence that is consistent with a concomitant proton transfer. We have found the process to be fully reversible and reproducible (see Figure 4 and Figure S7). This is an important observation that highlights possible functional differences between CbHydA1 and other [FeFe] hydrogenases and further motivates in-detail investigation. However, as the current work focuses on the process of inactivation, we consider this topic to be beyond the scope of this manuscript.

Protein film voltammetry (PFV). The unusually low inactivation-reactivation potential led us to test for possible catalytic bias and evidence of oxidative inactivation. For this purpose, we adsorbed *Cb*HydA1 directly onto a rotating pyrolytic-graphite electrode and performed cyclic voltammetry experiments under 1 atm H₂. In contrast to our expectations, the pH-dependent PFV experiments are consistent with a fully bidirectional enzyme. At basic pH, we observe lower H₂-reduction current and higher H₂-oxidation current and vice-versa for the acidic pH. For comparison, we also performed the experiments under limiting H₂ conditions and observed a subdued H₂ oxidation current, as expected (see Figure S8).

In agreement with the spectroelectrochemical experiments, we have observed inhibition of the oxidative catalytic current at mildly oxidizing potentials at all pH values tested. The low value of the inactivation potential is apparent in the hysteresis of the forward and reverse current at lower pH values. The apparent half-wave reactivation potential ($E_{\rm switch}$, see the insert to Figure 5 inset) appears much lower in CbHydA1 than in any other hydrogenases, including [NiFe] hydrogenases, obtained at similar experimental conditions (scan rate, electrode rotation speed, etc). $E_{\rm switch}$ is a kinetic parameter that only indirectly reflects the inactivation/reactivation potential⁴²; therefore, we refrain from a detailed analysis of this parameter here. Nonetheless, the observation of the $E_{\rm switch} <$ -200 mV at fairly fast scan rates (up to 100 mV/s was tested, see Figure S8) indicates that the enzyme quickly inactivates and reactivates at relatively low potentials. The low inactivation/reactivation potential observed is likely one of the key reasons for the efficacy of the O₂-protection mechanism.

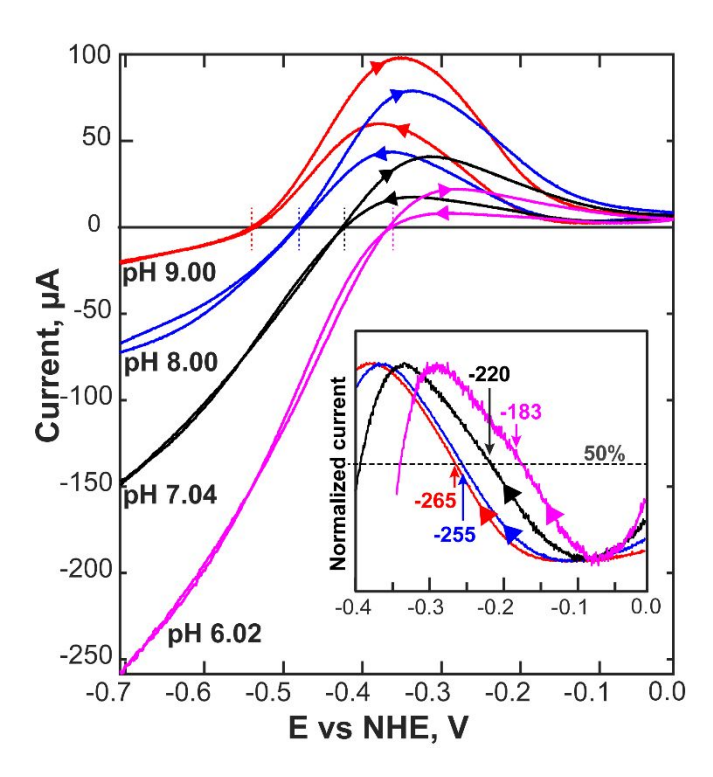


Figure 5. pH dependence of cyclic voltammetry experiments on CbHydA1 absorbed on a rotating disc graphite electrode under 1 atm H_2 . Dashed vertical lines indicate $2H^+/H_2$ equilibrium potential calculated for respective pH values at 1 atm H_2 . Inset shows the portions of the voltammograms (current normalized for clarity) corresponding to the reactivation process with arrows and numbers indicating estimated E_{switch} potential. Following color coding is used: red - pH 9.0, blue - pH 8.0, black - pH 7.04 and magenta - pH 6.02. All measurements were performed at 1000 RPM working electrode rotation rate, the temperature of 10 $^{\circ}$ C, and 10 mV/s scan rate.

Rodríguez-Maciá et al.⁶ observed a substantial decrease of the E_{switch} potential upon addition of Na₂S, indicating direct implication of sulfide in the process of inactivation. To verify the effect of Na₂S on inactivation/reactivation of CbHydA, we performed PFV experiments in the presence of 10mM Na₂S at 7.5 pH. The addition of Na₂S resulted in no apparent change in the PFV experiments (see Figure S9), thus confirming that sulfide does not affect the inactivation process of CbHydA.

Modeling the H_{inact} state. In the case of DdHydAB (and CrHydA1)⁶, the inactive state (H_{ox}^{air}) can be reversibly accessed if the sample solution contains Na₂S. It has been concluded that the H_{ox}^{air} contains an SH-ligand at the open coordination site, i.e. $[4Fe-4S]^{2+}-[Fe_p(II)-Fe_d(II)]-SH$ -core (see Figure 1).^{6,10} Considering that the IR bands for the H_{ox} and the $H_{red}H^+$ states are nearly identical between DdHydAB and CbHydA1 (see Table S1), we conclude that the protein environment and the structure of the H-cluster in the active state are very similar between the two enzymes. Despite the spectroscopic similarity of the active states, the CO-stretching IR bands of the H_{inact} state obtained in our study differ from the ones observed for H_{ox}^{air} in the DdHydAB by up to 9 cm⁻¹, indicating a somewhat different charge distribution around the H-cluster when in the O₂-protected state (see Table S1). The overall position of the IR bands, and the absence of an EPR signal are consistent with the $[4Fe-4S]^{2+}-[Fe_p(II)-Fe_d(II)]$ core of the H_{inact} state. However, the fact

that the presence of sulfide does not affect our PFV and IR experiments led us to conclude that the external ligand is not SH⁻ in the H_{inact} state observed in *Cb*HydA1.

Three different methods allowed us to obtain the same H_{inact} state: exposure to air, electrochemical oxidation under strictly anaerobic conditions, and using anaerobic chemical oxidation with HAR (see Figure 2). The fact that all methods result in the same H_{inact} state indicates that no uncommon exogenous molecule participates in the ligation of the inactive state. These findings exclude the possibility of molecular oxygen (or superoxide) as a ligand to the open coordination site. In addition, Mebs et al.²³ suggested that the $H_{ox}O_2$ state obtained by exposing C169A variant of CrHydA1 to air contains superoxide bound to diferrous [2Fe]_H. However, the FTIR spectra of $H_{ox}O_2$ are noticeably different from the ones observed in this study for the H_{inact} state (see Table S1) ruling out this possibility.

Density functional theory (DFT) can reproduce stretching vibration frequencies of the CO and CNligands of the H-cluster reasonably well.^{23,38}. Therefore, we conducted a set of DFT calculations to form a hypothesis for the identity of the ligand at the open coordination site of the H_{inact} state. Following the recent study by Mebs et al., 23, we adopted a full 6Fe-core model of the H-cluster. We used a broken symmetry approach to mimic the antiferromagnetic coupling between the two high-spin mixed-valent iron pairs (Fe(II)-Fe(III)) in the [4Fe-4S]_H cluster (see Figure S4). We also restricted our consideration to models consisting of low-spin di-ferrous [2Fe]_H subcluster (i.e. [Fe_p(II)-Fe_d(II)]). In our experience, the inclusion of the [4Fe-4S]_H subcluster to DFT models significantly improved the reproducibility of the CO stretch vibrations, especially of the bridging CO. Using this approach, we were able to reproduce, reasonably well, experimental IR data on the di-ferrous states such as H_{hyd} , H_{hyd}^{ODT} , 39 H_{ox}^{air} , 6 and $H_{ox}O_{2}^{23}$ states. Vibrational frequency calculations of the H_{ox} state resulted in a good fit to experimental data as well, confirming the viability of the used methodology. We calculated the combined root-mean-square deviation (RMSD) between experimental and calculated CO-stretch vibration frequencies to be 8.9 cm⁻¹. We will use this parameter as a rough borderline criterion (see Table S2 and Figure S10) for deciding fitness of modeled band positions to the experimental IR spectrum of the H_{inact} state.

We considered several likely models of the H_{inact} state based on experimental observations. Inspired by the Ni-B state of the [NiFe] hydrogenase and by early suggestions by Albracht et. al^{12,29} for the inactive state of *Dd*HydAB, we considered a possibility that a hydroxide ion is present at the open coordination site. We also considered water as a ligand as well as the model with the vacant open coordination site. Additionally, we considered a model where a cysteine side chain is coordinating the active center in the H_{inact} state due to the following argument. The presence of the H_{hyd} state in our spectroelectrochemical experiments highlights the possibility of a disrupted H⁺ transfer process. Based on the postulated catalytic mechanism (see Figure 1) hydride-bound diferrous state of the H-cluster is the last step in the reaction before the addition of a second H⁺ and subsequent release of the H₂ molecule. In the past, one possible way to obtain H_{hyd} was to replace the cysteine residue neighboring the ADT moiety with serine or alanine^{23,37}, effectively disrupting the H⁺-transfer pathway. To rationalize our observation of the H_{hyd} state in wild-type *Cb*HydA, we speculate that the sidechain of the conserved Cys367 is mobile, enabling rotation away from the optimum proton transfer position. Therefore, we considered a possibility that the Cys residue can

adopt a rotamer affording direct coordination to the Fe_d. In the absence of crystallographic data, we are not able to accurately model this scenario. Therefore, we included a simple [SCH₃-] model for the Cys367, and did not restrict its geometry during geometry optimization steps. Per discussion by Kubas et al.²⁷, we also included in our considerations the possibility that ROS-oxidized Cys367-sulfenic acid binds to Fe_d in either the protonated or deprotonated forms. Figure 6 shows the results of the calculations of these six models. We also included the superoxide-ligated model for completeness. For clarity, Figure 6 shows the RMSDs between frequencies of CO-stretch vibrations of the calculated models and the observed *Cb*HydA1 experimental values (accounting for the correction factor, see Figure S10). The complete table of calculated frequencies can be found in the supporting information (Table S2).

From the observations presented herein, it is apparent that the absence of a ligand at the open coordination site results in a significant shift of the IR bands in comparison to experimental data, suggesting this particular state is unlikely. Based on the outstanding differences between calculations and experiments, the $L = H_2O$ and the $L = OHSCH_3$ models are also implausible representations of this state. The addition of the superoxide is also not consistent with experimental results, as expected per the discussion above. However, both $L = OH^-$ and $L = OSCH_3^-$ models coincide with experimental data, as well as the "calibration" models of differous states match the corresponding experimental data.

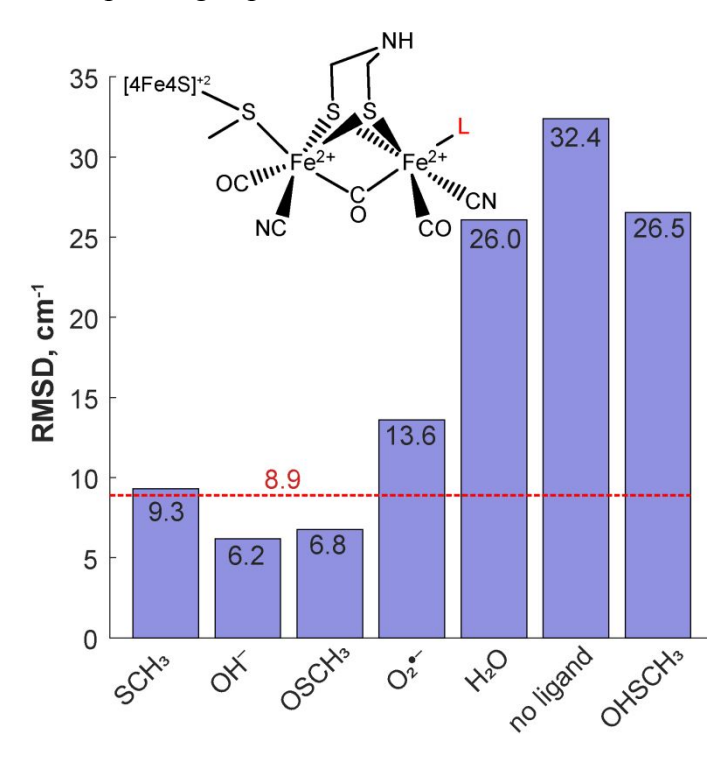


Figure 6. Root-Mean Square Deviation (RMSD) between CO-stretch vibration frequencies calculated for various H_{inact} models and experimentally observed values. Labels underneath the bars represent the identity of the L ligand shown in the insert. Red dashed line represents RMSD = 8.9 cm⁻¹ calculated between experimental and DFT-calculated IR frequencies for known states such as H_{ox} , H_{hyd} , H^{ODT}_{hyd} , H_{ox}^{air} and H_{ox} -O₂. Frequencies calculated for all models used can be found in the supporting information (see Table S1 and S2)

The $L = SCH_3$ (Cys) model obtained has a worse agreement to the experimental data of the H_{inact} than the $L = OH^-$ model (RMSD = 9.3 cm⁻¹ versus 6.2 cm⁻¹). Nonetheless, as the differences are only slightly outside our margins set by the reference RMSD (red line in Figure 6), we cannot conclusively dismiss this model. Hence, this analysis narrows down the most likely structures of the H_{inact} state to $L = OH^-$, $L = S^-$ -Cys and $L = OS^-$ -Cys models.

DISCUSSION

In this work, we observed that CbHydA1 is indeed an oxygen tolerant enzyme in the sense that it transitions to the O₂-protected H_{inact} state in the presence of O₂ and readily reactivates under reducing conditions. Rigorous removal of oxygen-reducing agents such as sodium dithionite and dithiothreitol did not alter the ability of CbHydA1 to tolerate oxygen. Based on the stability tests performed, we conclude that the partial loss of activity after prolonged O₂ exposure is likely due to overall protein stability and F-cluster degradation rather than due to the degradation of the Hcluster. An important difference between our work and the work performed by Morra et al. is that we utilized artificially activated enzymes using a synthetic [2Fe]_H precursor. Expressing apo-CbHydA1 instead of holo-CbHydA1 limits the possibility of an ROS-induced modification of the active cofactor environment via an H-cluster-assisted process (e.g., due to trace amounts of oxygen during isolation), such as the one observed for holo-CrHydA1 earlier ²⁶. Moreover, the absence of the effect of sulfide in our experiments indicates that the mechanism of inactivation and the identity of the H_{inact} state is different from the case of sulfide-dependent O₂-tolerance uncovered recently by Rodríguez-Maciá et al. for *Dd*HydAB and *Cr*HydA.^{6,10} Full reversibility of the inactivation process in spectro-electrochemical and PFV experiments also indicates that the H_{ox}-H_{inact} transition is not rate-limited by a diffusion of an external molecule. Therefore, we strongly suggest that the oxygen tolerance observed in CbHydA1 is an intrinsic property of the enzyme itself, rather than being induced by external factors.

Surprisingly, our spectroscopic analysis of the active states shows a high similarity between *Cb*HydA1 and other well-studied enzymes such as *Dd*HydAB and *Cr*HydA1. This fact indicates that the structure of the H-cluster and the surrounding protein environment itself are very similar between the aforementioned enzymes. This suggests that the oxygen tolerance observed in *Cb*HydA1 is unlikely to be due to peculiarities of the electronic structure of the active center itself. Also, our observations highlight the high conservation of the immediate protein scaffold around the [2Fe]_H and the [4Fe-4S]_H subclusters between *Cb*HydA1 and other [FeFe] hydrogenases. Strict conservation of the amino acid sequence in and around the H-cluster binding region between *Cb*HydA1 and other known [FeFe] hydrogenases supports this notion (see Figure S11).

While the structures of the H-cluster in the active states appears to be conserved, spectroelectrochemical titrations revealed important deviations in the electrochemical relationships between different states. We have observed an unexpected stabilization of the H_{hyd} state at low potentials even at relatively high pH 8.4. A more detailed investigation of this process is a matter of future research and is beyond the scope of this work. However, it is necessary to point out that the H_{hyd} state is not typically observed in conditions similar to the ones used in this work. To achieve accumulation of the H_{hyd} state, a proton-pathway disruption is required, which can be achieved by either using the inactive ODT-variant of the H-cluster³⁹ or amino acid

substitutions on the proton-pathway^{23,37} or using a combination of a low pH and a high H_2 concentration³⁷. Therefore, we speculate that the presence of H_{hyd} at neutral-to-high pH values in wild type CbHydA1 (prepared under 3% H_2) may indicate unusual flexibility in parts of the CbHydA1 protein folding associated with proton transfer pathway affording a proton transfer disruption. We consider the hypothesis that amino acid(s) in the vicinity of the H-cluster may effectively obstruct proton transfer. This notion led us to speculate that the Cys367 side chain may adopt a non-productive rotamer and thus to consider a possibility of Cys-S binding to the H-cluster in the inactive state, as discussed above.

Remarkably, the transition between the H_{ox} and the H_{inact} states occurs at an unusually low redox potential. In all our experiments, the inactivation potential is ≤ 100 mV than the $2H^+/H_2$ equilibrium potential. This relatively small gap is not only unusual for [FeFe] hydrogenases, but also for more O_2 -tolerant [NiFe] hydrogenases. Illustrative of this point is the comparison of the reactivation profiles in protein film voltammetry experiments. The mid-point potential of reactivation during the reductive CV sweep (E_{switch}), when taken at a similar pH and scan rate (10 mV/s) is at least 100 mV lower in the case of CbHydA1 than in [NiFe] hydrogenases (e.g. D. fructosovorans $E_{switch} \approx 0$ mV vs NHE at pH 6.1^{43} or D. fructosovorans V74N variant $E_{switch} \approx -60$ mV vs NHE at pH 5.5^{42} as compared to $E_{switch} \approx -180$ mV vs NHE at pH 6.04 for CbHydA). This difference reflects the higher efficiency of the inactivation process and thus higher oxygen tolerance of CbHydA. However, as E_{switch} is not a thermodynamic parameter and strongly depends on experimental conditions, a further side-by-side comparison is required to draw direct parallels.

In a recent publication, Esselborn et al.²⁵ illustrated that the oxidative degradation of the iron-sulfur clusters in CpI starts at the H-cluster. The absence of the [2Fe]_H subcluster resulted in no significant degradation of any of the clusters in CpI. This data corroborated an earlier report by Swanson et al. ²⁶ where a crystal structure of an O₂-exposed crystal of CrHydA showed evidence of cysteine sulfenic acid, which would be a result of oxidation by an ROS generated by the H-cluster. Throughout our experiments, we have not observed the typical H-cluster degradation product, H_{ox} -CO, which appears when free CO released from degraded H-cluster inhibits the still-intact enzyme molecules. Figure S12 illustrates an example of such a process in CpI: exposure to oxygen under similar conditions leads to the appearance of the H_{ox}-CO state before a complete disappearance of CO/CN⁻ signals from the IR spectrum between 2120 cm⁻¹ and 1780 cm⁻¹. In light of the recent Esselborn et al.²⁵ and Swanson et al.²⁶ reports, one can argue that the O₂-tolerance of CbHydA1 is due to the inability of O₂ molecules to enter the active site. However, Morra et al.³² reported that the exposure of the active enzyme to carbon monoxide leads to a full conversion of the active state to the H_{ox}-CO state. Our experiments confirm this result, illustrating the ability of diatomic molecules to enter the active site. Hence, we consider this scenario unlikely. Another critical observation is that CbHydA1 can be converted anaerobically to precisely the same H_{inact} state (electro)chemically. This observation suggests that the accumulation of the H_{inact} species is not dependent on the presence of oxygen, and can be obtained as a result of a simple redox transition.

We have formulated two hypotheses to rationalize these conclusions. Our first hypothesis is that the diffusion of O_2 to the H-cluster is much slower than the rate of diffusion of O_2 to the F-clusters. Consequently, the H-cluster oxidizes to the O_2 -protected H_{inact} state by the O_2 -oxidized F-clusters

before O_2 can interact with the active cofactor. Since our theoretical investigation strongly disfavors the vacant open coordination site model, the oxidation must proceed with the concomitant binding of a ligand. In turn, this unknown ligand must have a much higher binding affinity than O_2 since after 44 hours of exposure to air the H_{inact} spectrum remained unchanged, albeit with a 20% diminished intensity. We can exclude the possibility that the unidentified ligand is also present in the active states of the enzyme on the basis that the H_{ox} and $H_{red}H^+$ states observed in *in vitro* experiments are identical to those observed in DdHydAB, CrHydA, and CpI. It then follows that the binding of this additional ligand is concomitant with the (over)oxidation of the H-cluster. A key requirement of this mechanism is that the molecule that binds to the H-cluster must be readily available for efficient protection of the active site from O_2 binding. The two best-fitting DFT models of the H_{inact} state, $L = OH^-$ and $L = S^-$ -Cys, are consistent with this scenario. For the former to take place, a readily available water molecule must exist in the active-site pocket. For the latter, the Cys367 residue near Fe_d must reside on a very mobile flexible loop and have a high probability of rotating its side chain towards the open coordination site to afford coordination.

An alternative hypothesis is that O_2 is reduced by the H-cluster, resulting in a state identical to what can be obtained from anaerobic (electro)chemical oxidation. For example, such a scenario is observed in [NiFe] hydrogenases. The Ni-B state, a hydroxide-bound state, can be obtained by reduction of oxygen at the [NiFe] metallocofactor, or anaerobically in electrochemical experiments. Kubas et al.²⁷ proposed the possibility of a safe reaction of the H-cluster with oxygen in an electron-rich environment. When enough electrons and protons are available, the $[2Fe(II)]_H$ -OH⁻ + H₂O state is one of the plausible outcomes of O₂-reduction by the active site. Under anaerobic conditions, water can be deprotonated (perhaps by Cys367) to produce the same $[2Fe(II)]_H$ -OH⁻ state of the $[2Fe]_H$.

Lastly, Kubas et al.²⁷ also proposed that ROS can oxidize the Cys residue to sulfenic acid (Cys-S-OH) in the process of O₂ reduction. Therefore, it seems feasible that the Cys-sulfenic acid generated through the oxidation of cysteine can then bind to the open coordination site. Our DFT calculations support this as a viable possibility. However, the generation of such a species requires reaction with oxygen and should not be possible otherwise. Since we expressed and isolated *Cb*HydA1 anaerobically in the apo form, we can exclude oxidation of the cysteine during sample preparation. Therefore, based on the fact that we are able to generate the H_{inact} state anaerobically, we rule out this scenario.

To summarize the discussion above, we propose that the H_{inact} state consists of a diamagnetic [4Fe-4S]_H²⁺-[2Fe(II)]_H core retaining its usual CO/CN⁻ coordination and the open coordination site is occupied by either OH⁻ or by an S⁻-Cys ligand (see Scheme 1).

Scheme 1.

The efficiency of oxidative inactivation displayed in our electrochemical experiments is another unusual property of CbHydA1. We observed that CbHydA1 converts to the O_2 -tolerant inactive state under what in case of [NiFe] hydrogenases would be considered a mildly reducing condition. In accordance, we have illustrated that treating CbHydA1 with a low-potential mediator such as neutral red ($E_0 = -363$ mV vs. NHE at pH 7.4) is sufficient to reach an equilibrium between the H_{inact} state and the H_{ox} state. These data indicate that the inactivation is thermodynamically favorable under mildly oxidizing conditions (with respect to the $2H^+/H_2$ midpoint potential).

In this respect, it is rather intriguing that the immediate amino acid framework around the H-cluster is fairly well conserved (see Figure S11). In the absence of x-ray crystallographic data, we cannot rule out major changes to the overall structure of the protein environment dictated by the second sphere of amino acids. However, the fact that the active states of the H-cluster (H_{ox} and H_{red}H⁺) have a striking spectroscopic resemblance to the same states observed in other [FeFe] hydrogenases highlights structural conservation of the H-cluster binding pocket.

On the other hand, we observed a substantial difference in the residue content around the F-clusters (see Figure S11). In *Cb*HydA1, the amino acids neighboring the proximal F-cluster are substantially more polar. Hence, the electronic properties of the F-cluster may play a role in imparting oxygen tolerance in this system. Future experiments targeting the redox properties of the F-cluster should clarify this point.

Lastly, *Clostridium beijerinckii* is a strictly anaerobic bacterium with the useful ability to produce such solvents as butanol, acetone, ethanol and isopropanol under anaerobic conditions. ^{44–46} The exact physiological function of *Cb*HydA1 is unresolved. The fact that the *Cb*HydA1 and close homologues have expression profiles matching the H₂ release profile (maximized during cell growth and proliferation) leads to the suggestion that this enzyme acts as an electron sink on the pyruvate to acetyl-CoA conversion pathway. ^{47,48} If this hypothesis holds true, then the function of *Cb*HydA1 is similar to that of CpI in *C.pasteurianum*. ⁴⁹ However, while PFV experiments of *Cp*I indicate an expected bias towards hydrogen production, our experiment show bi-direction nature of *Cb*HydA1. Is it possible that the inactivation under mildly electron-poor conditions is an alternative (to *Cp*I) regulatory mechanism to inhibit the enzyme's function in the absence of

reduced ferredoxins? Further studies into metabolisms of *C.beijerinkii* are needed to clarify this intriguing possibility. If this is the case, O₂-tolerance of *Cb*HydA1 can be a fortunate consequence of this regulatory property.

CONCLUSIONS

Our work highlights the unprecedented oxygen tolerance of *Cb*HydA. Our data indicate that in the presence of oxygen, the enzyme enters an inactive state regardless of the presence of sulfides or sodium dithionite. The same H_{inact} state can also be obtained by oxidation chemically or electrochemically. The inactivation occurs at rather low potentials, which partially explains the efficiency of the inactivation process. The data presented indicate the presence of a readily-available ligand (either side-chain of Cys or hydroxide) that coordinates the active site under mildly oxidizing conditions, leading to the O₂-protected state. The exceptional ability of *Cb*HydA1 to remain highly stable in the presence of high concentrations of oxygen and to be able to reactivate under reducing conditions provides an unprecedented opportunity to utilized [FeFe] hydrogenases in biotechnological applications in the future.

ACKNOWLEDGMENTS

The authors thank Prof. John Golbeck for the kind gift of *CpI* plasmid and BL21 Δ*icr E.coli* strain. This work was supported by the National Science Foundation (CHE-1943748) and the U.S. Department of Energy (DE-FG-02-05-ER46222).

ASSOCIATE CONTENT

The Supporting information is available free of charge on ACS Publication Website.

Supporting information contains materials and methods, additional details of the experimental setup and theoretical methods, results of H₂ oxidation activity assays, EPR and FTIR spectra of *Cb*HydA1 before and after O₂ exposure, FTIR spectroelectrochemistry of *Cb*HydA1 at pH7.4, Protein film voltammetry, tables with experimental and theoretical IR data, sequence alignment between various [FeFe] hydrogenases, FTIR spectra of *Cp*I.

AUTHOR INFORMATION

* Alexey Silakov, E-mail: aus40@psu.edu; Telephone: +1 (814) 863-7248

REFERENCES

- (1) Kalamaras, C. M.; Efstathiou, A. M. Hydrogen Production Technologies: Current State and Future Developments. *Conference Papers in Energy* **2013**, *2013*, 1–9. https://doi.org/10.1155/2013/690627.
- (2) Lubitz, W.; Ogata, H.; Rüdiger, O.; Reijerse, E. Hydrogenases. *Chem. Rev.* **2014**, *114* (8), 4081–4148. https://doi.org/10.1021/cr4005814.
- (3) Madden, C.; Vaughn, M. D.; Díez-Pérez, I.; Brown, K. A.; King, P. W.; Gust, D.; Moore, A. L.; Moore, T. A. Catalytic Turnover of [FeFe]-Hydrogenase Based on Single-Molecule Imaging. *J. Am. Chem. Soc.* **2012**, *134* (3), 1577–1582. https://doi.org/10.1021/ja207461t.
- (4) Pandey, K.; Islam, S. T. A.; Happe, T.; Armstrong, F. A. Frequency and Potential Dependence of Reversible Electrocatalytic Hydrogen Interconversion by [FeFe]-Hydrogenases. *Proc. Natl. Acad. Sci. U.S.A.* **2017**, *114* (15), 3843–3848. https://doi.org/10.1073/pnas.1619961114.

- (5) Birrell, J. A.; Wrede, K.; Pawlak, K.; Rodriguez-Maciá, P.; Rüdiger, O.; Reijerse, E. J.; Lubitz, W. Artificial Maturation of the Highly Active Heterodimeric [FeFe] Hydrogenase from *Desulfovibrio Desulfuricans* ATCC 7757. *Isr. J. Chem.* **2016**, *56* (9–10), 852–863. https://doi.org/10.1002/ijch.201600035.
- (6) Rodríguez-Maciá, P.; Reijerse, E. J.; van Gastel, M.; DeBeer, S.; Lubitz, W.; Rüdiger, O.; Birrell, J. A. Sulfide Protects [FeFe] Hydrogenases From O₂. *J. Am. Chem. Soc.* **2018**, *140* (30), 9346–9350. https://doi.org/10.1021/jacs.8b04339.
- (7) Rodríguez-Maciá, P.; Pawlak, K.; Rüdiger, O.; Reijerse, E. J.; Lubitz, W.; Birrell, J. A. Intercluster Redox Coupling Influences Protonation at the H-Cluster in [FeFe] Hydrogenases. *J. Am. Chem. Soc.* **2017**, *139* (42), 15122–15134. https://doi.org/10.1021/jacs.7b08193.
- (8) Sommer, C.; Adamska-Venkatesh, A.; Pawlak, K.; Birrell, J. A.; Rüdiger, O.; Reijerse, E. J.; Lubitz, W. Proton Coupled Electronic Rearrangement within the H-Cluster as an Essential Step in the Catalytic Cycle of [FeFe] Hydrogenases. *J. Am. Chem. Soc.* **2017**, *139* (4), 1440–1443. https://doi.org/10.1021/jacs.6b12636.
- (9) Lorent, C.; Katz, S.; Duan, J.; Kulka, C. J.; Caserta, G.; Teutloff, C.; Yadav, S.; Apfel, U.-P.; Winkler, M.; Happe, T.; Horch, M.; Zebger, I. Shedding Light on Proton and Electron Dynamics in [FeFe] Hydrogenases. *J. Am. Chem. Soc.* 2020, 142 (12), 5493–5497. https://doi.org/10.1021/jacs.9b13075.
- (10) Rodríguez-Maciá, P.; Galle, L.; Bjornsson, R.; Lorent, C.; Zebger, I.; Yoda, Y.; Cramer, S.; DeBeer, S.; Span, I.; Birrell, J. Caught in the Hinact: Crystal Structure and Spectroscopy Reveal a Sulfur Bound to the Active Site of an O2-stable State of [FeFe] Hydrogenase. *Angew. Chem. Int. Ed.* **2020**, anie.202005208. https://doi.org/10.1002/anie.202005208.
- (11) Silakov, A.; Reijerse, E. J.; Albracht, S. P. J.; Hatchikian, E. C.; Lubitz, W. The Electronic Structure of the H-Cluster in the [FeFe]-Hydrogenase from *Desulfovibrio Desulfuricans*: A Q-Band ⁵⁷Fe-ENDOR and HYSCORE Study. *J. Am. Chem. Soc.* **2007**, *129* (37), 11447–11458. https://doi.org/10.1021/ja072592s.
- (12) Roseboom, W.; De Lacey, A. L.; Fernandez, V. M.; Hatchikian, E. C.; Albracht, S. P. J. The Active Site of the [FeFe]-Hydrogenase from *Desulfovibrio Desulfuricans*. II. Redox Properties, Light Sensitivity and CO-Ligand Exchange as Observed by Infrared Spectroscopy. *J. Biol. Inorg. Chem.* **2006**, *11* (1), 102–118. https://doi.org/10.1007/s00775-005-0040-2.
- (13) Adamska-Venkatesh, A.; Roy, S.; Siebel, J. F.; Simmons, T. R.; Fontecave, M.; Artero, V.; Reijerse, E.; Lubitz, W. Spectroscopic Characterization of the Bridging Amine in the Active Site of [FeFe] Hydrogenase Using Isotopologues of the H-Cluster. *J. Am. Chem. Soc.* **2015**, *137* (40), 12744–12747. https://doi.org/10.1021/jacs.5b06240.
- (14) Silakov, A.; Wenk, B.; Reijerse, E.; Lubitz, W. ¹⁴N HYSCORE Investigation of the H-Cluster of [FeFe] Hydrogenase: Evidence for a Nitrogen in the Dithiol Bridge. *Phys. Chem. Chem. Phys.* **2009**, *11* (31), 6592. https://doi.org/10.1039/b905841a.
- (15) Byer, A. S.; Shepard, E. M.; Ratzloff, M. W.; Betz, J. N.; King, P. W.; Broderick, W. E.; Broderick, J. B. H-Cluster Assembly Intermediates Built on HydF by the Radical SAM Enzymes HydE and HydG. *J. Biol. Inorg. Chem.* 2019, 24 (6), 783–792. https://doi.org/10.1007/s00775-019-01709-7.
- (16) Caserta, G.; Pecqueur, L.; Adamska-Venkatesh, A.; Papini, C.; Roy, S.; Artero, V.; Atta, M.; Reijerse, E.; Lubitz, W.; Fontecave, M. Structural and Functional Characterization of the Hydrogenase-Maturation HydF Protein. *Nat. Chem. Biol.* **2017**, *13* (7), 779–784. https://doi.org/10.1038/nchembio.2385.
- (17) Kuchenreuther, J. M.; George, S. J.; Grady-Smith, C. S.; Cramer, S. P.; Swartz, J. R. Cell-Free H-Cluster Synthesis and [FeFe] Hydrogenase Activation: All Five CO and CN—Ligands Derive from Tyrosine. *PLoS ONE* **2011**, *6* (5), e20346. https://doi.org/10.1371/journal.pone.0020346.
- (18) Rao, G.; Tao, L.; Britt, R. D. Serine Is the Molecular Source of the NH(CH₂)₂ Bridgehead Moiety of the *in Vitro* Assembled [FeFe] Hydrogenase H-Cluster. *Chem. Sci.* **2020**, *11* (5), 1241–1247. https://doi.org/10.1039/C9SC05900H.

- (19) Lampret, O.; Esselborn, J.; Haas, R.; Rutz, A.; Booth, R. L.; Kertess, L.; Wittkamp, F.; Megarity, C. F.; Armstrong, F. A.; Winkler, M.; Happe, T. The Final Steps of [FeFe]-Hydrogenase Maturation. *Proc. Natl. Acad. Sci. U.S.A.* 2019, *116* (32), 15802–15810. https://doi.org/10.1073/pnas.1908121116.
- (20) Suess, D. L. M.; Pham, C. C.; Bürstel, I.; Swartz, J. R.; Cramer, S. P.; Britt, R. D. The Radical SAM Enzyme HydG Requires Cysteine and a Dangler Iron for Generating an Organometallic Precursor to the [FeFe]-Hydrogenase H-Cluster. *J. Am. Chem. Soc.* **2016**, *138* (4), 1146–1149. https://doi.org/10.1021/jacs.5b12512.
- (21) Esselborn, J.; Lambertz, C.; Adamska-Venkatesh, A.; Simmons, T.; Berggren, G.; Noth, J.; Siebel, J.; Hemschemeier, A.; Artero, V.; Reijerse, E.; Fontecave, M.; Lubitz, W.; Happe, T. Spontaneous Activation of [FeFe]-Hydrogenases by an Inorganic [2Fe] Active Site Mimic. *Nat. Chem. Biol.* **2013**, *9* (10), 607–609. https://doi.org/10.1038/nchembio.1311.
- (22) Berggren, G.; Adamska, A.; Lambertz, C.; Simmons, T. R.; Esselborn, J.; Atta, M.; Gambarelli, S.; Mouesca, J.-M.; Reijerse, E.; Lubitz, W.; Happe, T.; Artero, V.; Fontecave, M. Biomimetic Assembly and Activation of [FeFe]-Hydrogenases. *Nature* **2013**, *499* (7456), 66–69. https://doi.org/10.1038/nature12239.
- (23) Mebs, S.; Kositzki, R.; Duan, J.; Kertess, L.; Senger, M.; Wittkamp, F.; Apfel, U.-P.; Happe, T.; Stripp, S. T.; Winkler, M.; Haumann, M. Hydrogen and Oxygen Trapping at the H-Cluster of [FeFe]-Hydrogenase Revealed by Site-Selective Spectroscopy and QM/MM Calculations. *Biochim. Biophys. Acta, Bioenerg.* **2018**, *1859* (1), 28–41. https://doi.org/10.1016/j.bbabio.2017.09.003.
- (24) Noth, J.; Esselborn, J.; Güldenhaupt, J.; Brünje, A.; Sawyer, A.; Apfel, U.-P.; Gerwert, K.; Hofmann, E.; Winkler, M.; Happe, T. [FeFe]-Hydrogenase with Chalcogenide Substitutions at the H-Cluster Maintains Full H₂ Evolution Activity. *Angew. Chem. Int. Ed.* **2016**, *55* (29), 8396–8400. https://doi.org/10.1002/anie.201511896.
- (25) Esselborn, J.; Kertess, L.; Apfel, U.-P.; Hofmann, E.; Happe, T. Loss of Specific Active-Site Iron Atoms in Oxygen-Exposed [FeFe]-Hydrogenase Determined by Detailed X-Ray Structure Analyses. *J. Am. Chem. Soc.* **2019**, *141* (44), 17721–17728. https://doi.org/10.1021/jacs.9b07808.
- (26) Swanson, K. D.; Ratzloff, M. W.; Mulder, D. W.; Artz, J. H.; Ghose, S.; Hoffman, A.; White, S.; Zadvornyy, O. A.; Broderick, J. B.; Bothner, B.; King, P. W.; Peters, J. W. [FeFe]-Hydrogenase Oxygen Inactivation Is Initiated at the H Cluster 2Fe Subcluster. *J. Am. Chem. Soc.* **2015**, *137* (5), 1809–1816. https://doi.org/10.1021/ja510169s.
- (27) Kubas, A.; Orain, C.; De Sancho, D.; Saujet, L.; Sensi, M.; Gauquelin, C.; Meynial-Salles, I.; Soucaille, P.; Bottin, H.; Baffert, C.; Fourmond, V.; Best, R. B.; Blumberger, J.; Léger, C. Mechanism of O₂ Diffusion and Reduction in FeFe Hydrogenases. *Nature Chem.* **2017**, *9* (1), 88–95. https://doi.org/10.1038/nchem.2592.
- (28) Lambertz, C.; Leidel, N.; Havelius, K. G. V.; Noth, J.; Chernev, P.; Winkler, M.; Happe, T.; Haumann, M. O₂ Reactions at the Six-Iron Active Site (H-Cluster) in [FeFe]-Hydrogenase. *J. Biol. Chem.* **2011**, *286* (47), 40614–40623. https://doi.org/10.1074/jbc.M111.283648.
- (29) Albracht, S. P. J.; Roseboom, W.; Hatchikian, E. C. The Active Site of the [FeFe]-Hydrogenase from *Desulfovibrio Desulfuricans*. I. Light Sensitivity and Magnetic Hyperfine Interactions as Observed by Electron Paramagnetic Resonance. *J. Biol. Inorg. Chem.* **2006**, *11* (1), 88–101. https://doi.org/10.1007/s00775-005-0039-8.
- (30) Baffert, C.; Demuez, M.; Cournac, L.; Burlat, B.; Guigliarelli, B.; Bertrand, P.; Girbal, L.; Léger, C. Hydrogen-Activating Enzymes: Activity Does Not Correlate with Oxygen Sensitivity. *Angew. Chem. Int. Ed.* **2008**, *47* (11), 2052–2054. https://doi.org/10.1002/anie.200704313.
- (31) Caserta, G.; Papini, C.; Adamska-Venkatesh, A.; Pecqueur, L.; Sommer, C.; Reijerse, E.; Lubitz, W.; Gauquelin, C.; Meynial-Salles, I.; Pramanik, D.; Artero, V.; Atta, M.; del Barrio, M.; Faivre, B.; Fourmond, V.; Léger, C.; Fontecave, M. Engineering an [FeFe]-Hydrogenase: Do Accessory Clusters Influence O₂ Resistance and Catalytic Bias? *J. Am. Chem. Soc.* **2018**, *140* (16), 5516–5526. https://doi.org/10.1021/jacs.8b01689.

- (32) Morra, S.; Arizzi, M.; Valetti, F.; Gilardi, G. Oxygen Stability in the New [FeFe]-Hydrogenase from *Clostridium Beijerinckii* SM10 (CbA5H). *Biochemistry* **2016**, *55* (42), 5897–5900. https://doi.org/10.1021/acs.biochem.6b00780.
- (33) Birrell, J. A.; Pelmenschikov, V.; Mishra, N.; Wang, H.; Yoda, Y.; Tamasaku, K.; Rauchfuss, T. B.; Cramer, S. P.; Lubitz, W.; DeBeer, S. Spectroscopic and Computational Evidence That [FeFe] Hydrogenases Operate Exclusively with CO-Bridged Intermediates. *J. Am. Chem. Soc.* **2020**, *142* (1), 222–232. https://doi.org/10.1021/jacs.9b09745.
- (34) Guigliarelli, B.; Bertrand, P. Application of EPR Spectroscopy to the Structural and Functional Study of Iron-Sulfur Proteins. In *Advances in Inorganic Chemistry*; Elsevier, 1999; Vol. 47, pp 421–497. https://doi.org/10.1016/S0898-8838(08)60084-7.
- (35) Rodríguez-Maciá, P.; Birrell, J. A.; Lubitz, W.; Rüdiger, O. Electrochemical Investigations on the Inactivation of the [FeFe] Hydrogenase from *Desulfovibrio Desulfuricans* by O ₂ or Light under Hydrogen-Producing Conditions. *ChemPlusChem* **2017**, *82* (4), 540–545. https://doi.org/10.1002/cplu.201600508.
- (36) Stripp, S. T.; Goldet, G.; Brandmayr, C.; Sanganas, O.; Vincent, K. A.; Haumann, M.; Armstrong, F. A.; Happe, T. How Oxygen Attacks [FeFe] Hydrogenases from Photosynthetic Organisms. *Proc. Natl. Acad. Sci. U.S.A.* **2009**, *106* (41), 17331–17336. https://doi.org/10.1073/pnas.0905343106.
- (37) Winkler, M.; Senger, M.; Duan, J.; Esselborn, J.; Wittkamp, F.; Hofmann, E.; Apfel, U.-P.; Stripp, S. T.; Happe, T. Accumulating the Hydride State in the Catalytic Cycle of [FeFe]-Hydrogenases. *Nat. Commun.* **2017**, *8* (1), 16115. https://doi.org/10.1038/ncomms16115.
- (38) Mulder, D. W.; Guo, Y.; Ratzloff, M. W.; King, P. W. Identification of a Catalytic Iron-Hydride at the H-Cluster of [FeFe]-Hydrogenase. *J. Am. Chem. Soc.* **2017**, *139* (1), 83–86. https://doi.org/10.1021/jacs.6b11409.
- (39) Reijerse, E. J.; Pham, C. C.; Pelmenschikov, V.; Gilbert-Wilson, R.; Adamska-Venkatesh, A.; Siebel, J. F.; Gee, L. B.; Yoda, Y.; Tamasaku, K.; Lubitz, W.; Rauchfuss, T. B.; Cramer, S. P. Direct Observation of an Iron-Bound Terminal Hydride in [FeFe]-Hydrogenase by Nuclear Resonance Vibrational Spectroscopy. *J. Am. Chem. Soc.* **2017**, *139* (12), 4306–4309. https://doi.org/10.1021/jacs.7b00686.
- (40) Oldham, K. B. The Potential-Dependence of Electrochemical Rate Constants. *J. Electroanal. Chem. Interf. Electrochem.* **1968**, *16* (2), 125–130. https://doi.org/10.1016/S0022-0728(68)80054-3.
- (41) Adamska, A.; Silakov, A.; Lambertz, C.; Rüdiger, O.; Happe, T.; Reijerse, E.; Lubitz, W. Identification and Characterization of the "Super-Reduced" State of the H-Cluster in [FeFe] Hydrogenase: A New Building Block for the Catalytic Cycle? *Angew. Chem. Int. Ed.* **2012**, *51* (46), 11458–11462. https://doi.org/10.1002/anie.201204800.
- (42) Abou Hamdan, A.; Liebgott, P.-P.; Fourmond, V.; Gutierrez-Sanz, O.; De Lacey, A. L.; Infossi, P.; Rousset, M.; Dementin, S.; Leger, C. Relation between Anaerobic Inactivation and Oxygen Tolerance in a Large Series of NiFe Hydrogenase Mutants. *Proc. Natl. Acad. Sci. U.S.A.* **2012**, *109* (49), 19916–19921. https://doi.org/10.1073/pnas.1212258109.
- (43) Fourmond, V.; Infossi, P.; Giudici-Orticoni, M.-T.; Bertrand, P.; Léger, C. "Two-Step" Chronoamperometric Method for Studying the Anaerobic Inactivation of an Oxygen Tolerant NiFe Hydrogenase. *J. Am. Chem. Soc.* **2010**, *132* (13), 4848–4857. https://doi.org/10.1021/ja910685j.
- (44) Zhang, C.; Li, T.; He, J. Characterization and Genome Analysis of a Butanol–Isopropanol-Producing Clostridium Beijerinckii Strain BGS1. *Biotechnol Biofuels* **2018**, *11* (1), 280. https://doi.org/10.1186/s13068-018-1274-x.
- (45) Chen, J.-S.; Hiu, S. F. Acetone-Butanol-Isopropanol Production ByClostridium Beijerinckii (Synonym,Clostridium Butylicum). *Biotechnol Lett* **1986**, *8* (5), 371–376. https://doi.org/10.1007/BF01040869.

- (46) Lépiz-Aguilar, L. Acetone-Butanol-Ethanol (ABE) Production in Fermentation of Enzymatically Hydrolyzed Cassava Flour by Clostridium Beijerinckii BA101 and Solvent Separation. *J. Microbiol. Biotechnol.* **2013**, *23* (8), 1092–1098. https://doi.org/10.4014/jmb.1301.01021.
- (47) Patakova, P.; Branska, B.; Sedlar, K.; Vasylkivska, M.; Jureckova, K.; Kolek, J.; Koscova, P.; Provaznik, I. Acidogenesis, Solventogenesis, Metabolic Stress Response and Life Cycle Changes in Clostridium Beijerinckii NRRL B-598 at the Transcriptomic Level. *Sci Rep* **2019**, *9* (1), 1371. https://doi.org/10.1038/s41598-018-37679-0.
- (48) Morra, S.; Arizzi, M.; Allegra, P.; La Licata, B.; Sagnelli, F.; Zitella, P.; Gilardi, G.; Valetti, F. Expression of Different Types of [FeFe]-Hydrogenase Genes in Bacteria Isolated from a Population of a Bio-Hydrogen Pilot-Scale Plant. *International Journal of Hydrogen Energy* **2014**, 39 (17), 9018–9027. https://doi.org/10.1016/j.ijhydene.2014.04.009.
- (49) Therien, J. B.; Artz, J. H.; Poudel, S.; Hamilton, T. L.; Liu, Z.; Noone, S. M.; Adams, M. W. W.; King, P. W.; Bryant, D. A.; Boyd, E. S.; Peters, J. W. The Physiological Functions and Structural Determinants of Catalytic Bias in the [FeFe]-Hydrogenases CpI and CpII of Clostridium Pasteurianum Strain W5. *Front. Microbiol.* **2017**, *8*, 1305. https://doi.org/10.3389/fmicb.2017.01305.

FOR TABLE OF CONTENTS ONLY

